Simulation of Finite-Size Photonic Crystal Surface Emitting Lasers with Efficient Eigenmode Solver

Yuan-Chun Han
Institute of Electronics
National Yang Ming Chiao Tung University
Hsinchu City 30010, Taiwan
ychan.stanley.ee12@nycu.edu.tw

Gray Lin
Institute of Electronics
National Yang Ming Chiao Tung University
Hsinchu City 30010, Taiwan
graylin@nycu.edu.tw

***Abstract*—We present an efficient eigenmode solver to simulate finite-size photonic-crystal (PC) surface-emitting lasers. Instead of calculating the full eigenspectra, a number of modes with lowest modal losses are extracted from the Krylov-Schur method and refined further using the shifted inverse power method. The device characteristics are then calculated and analyzed in terms of cavity size and PC fill factor.**

***Index Terms*—Photonic Crystals, Surface-Emitting Lasers, Coupled Wave Theory, Krylov-Schur Method, Shifted Inverse Power Method**

I. Introduction

The potential of photonic-crystal (PC) surface-emitting lasers (SELs) has been demonstrated by their high output power and narrow beam divergence. These properties make them suitable for applications in free-space optical communication, light detection and ranging [1] . However, continuing progress toward optimization is not an easy task. To avoid aimless test, simulation should be submitted as an exploratory tool at an early stage.

Due to limitations in computational resources, three-dimensional (3D) coupled wave theory (CWT) is introduced to model PCSEL devices [2]. In simulating infinite PC cavity, solving the basic eigenmodes is trivial, while in finite-size cavity with large area or large grid number, solving a huge number of eigenmodes is time-consuming. Therefore, it is formidable to investigate the dependence of parameters in addition to cavity size on device behaviors.

This paper presents an efficient eigenmode solver for finite-size PCSEL devices in the 3D-CWT formulation. The hybrid iterative approach combines the shift-and-invert Krylov-Schur method (KSM) [3] and the shifted inverse power method (SIPM), which enables identification of the lowest-loss modes for iterative refinement in an efficient and accurate manner. This is important for the subsequent analysis of surface emission characteristics.

II. Simulation Details

A. Device Structure

Fig. 1 shows the schematic of PCSEL device in the 940 nm wavelength range. The air-pillar PC structure is incorporated by deeply etching the topmost layers and no epitaxial regrowth is required [4]. In this simulation, square-latticed photonic crystals patterned in the shape of a right-isosceles triangle (RIT) are assumed. Moreover, the 400-nm thin-cladding layer is completely etched to maximize the diffraction coupling.

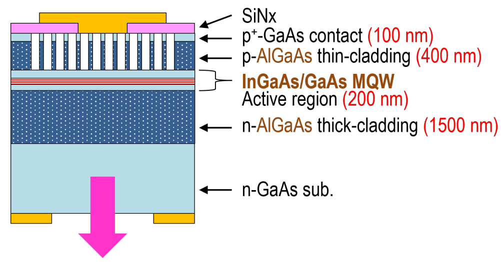

Fig. 1: Air-pillar PCSEL device under simulation

B. Coupled-Wave Model

In 3D-CWT model, the field profile in the z direction is decoupled from the in-plane profile and solved by the transfer matrix method. Four basic waves of R_x, S_x, R_y, and S_y represent the field amplitudes in the $+x$, $-x$, $+y$, and $-y$ directions, respectively. The coupled wave equations formulated in matrix form are given as,

$$(\delta + i\frac{\alpha}{2})\begin{pmatrix} R_x \\ S_x \\ R_y \\ S_y \end{pmatrix} = C\begin{pmatrix} R_x \\ S_x \\ R_y \\ S_y \end{pmatrix} + i\begin{pmatrix} \partial R_x/\partial x \\ -\partial S_x/\partial x \\ \partial R_y/\partial y \\ -\partial S_y/\partial y \end{pmatrix} \quad (1)$$

where C is the coupling matrix as derived in [3], δ is the normalized frequency detuning and α is the modal power losses, including surface radiation loss (α_{rad}) and edge loss (α_{edge}). The above threshold slope efficiency (S.E.) can be estimated according to the formula,

$$S.E. \approx \frac{1.24}{\lambda_0}\frac{(1/2)\alpha_{rad}}{\alpha_{rad}+\alpha_{edge}+\alpha_{int}}\left(\frac{W}{A}\right) \quad (2)$$

where λ_0 is lasing wavelength in μm and α_{int} is internal power loss of 5 cm^{-1} [4]. The factor $1/2$ assumes that only downward emissions contribute to the optical output.

C. Numerical Methods

To simulate PCSEL in a finite-size area, the laser cavity is discretized into $N \times N$ mesh grids where appropriate boundary conditions are imposed [2]. The 3D-CWT matrix in Eqn. 1 is then transformed into the eigenvalue problem of a large sparse matrix $(4N^2 \times 4N^2)$. Our proposed approach for the large eigenproblem is to apply the KSM in combination with the SIPM. The KSM requires a reduced time frame to obtain, for example, $N/2, N$ or $2N$ approximate eigenvalues with lowest modal losses. Afterward, the SIPM is iterated to refine the accurate and precise eigenmodes.

III. Results and Discussions

A. Simulation Time

The simulation time of three eigenmode solvers was compared: Schur decomposition, KSM, and KSM+SIPM. As shown in Fig. 2, Schur decomposition is the most time consuming, while KSM follows closely behind. In contrast, KSM+SIPM solver requires less than half the time of the former approach. However, KSM+SIPM solver is subject to variation in simulation times, depending on how many approximated eigenvalues are selected for iterative refinement. Considering a laser cavity of $400 \times 400\ \mu m^2$ discretized to mesh grids of 51×51 ($N = 51, \Delta x = \Delta y \approx 7.84\ \mu m$), the simulation time using KSM+SIPM is reduced to one-seventh of that using Schur or KSM.

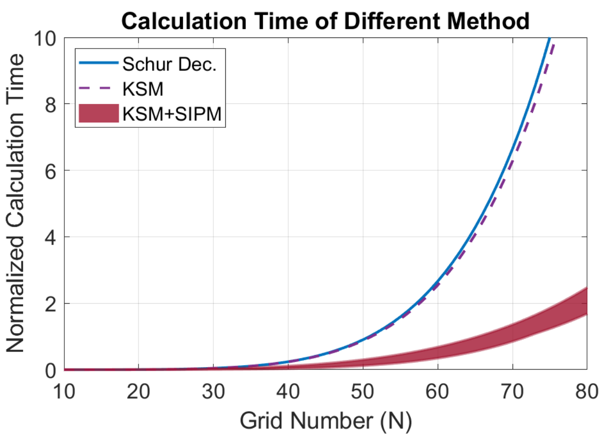

Fig. 2: The normalized simulation time of eigenmode solvers.

B. Cavity Design and FF Dependence

To demonstrate the powerful eigenmode solver, various emission characteristics of modal frequency, modal loss, slope efficiency, and loss discrimination are calculated and analyzed in terms of cavity size and fill factor (FF) as shown in Fig. 3.

In Fig. 3a, higher slope efficiency is observed in cavity sizes between 200 μm and 400 μm, with FF ranging from 18 % to 30 %. Focusing on the region of interest in Fig. 3c, total modal losses are not the lowest, but acceptable for high-power applications. Notably, a change or switch in frequency detuning can be observed in Fig. 3b. In fact, we have observed this modal frequency switch between modes A and B at $FF \approx 25\%$ in the analysis of infinite-cavity RIT-PCSELs [4]. It is interesting that in a finite-size cavity, the modal frequency switches at lower FF and increases with cavity size, as shown in Fig. 3c. Besides, the mode switching indicates that there is change in total losses, i.e. loss discrimination is minimized, which results in multi-mode emissions. Therefore, the loss discrimination minimum, corresponding to the dark line in Fig. 3d, should be excluded in the design of single-mode emissions.

In summary, there are two windows for fabrication design,

1) FF $= 18 - 20\%$ with cavity size $280 - 320\ \mu m$
2) FF $= 25 - 30\%$ with cavity size $200 - 250\ \mu m$

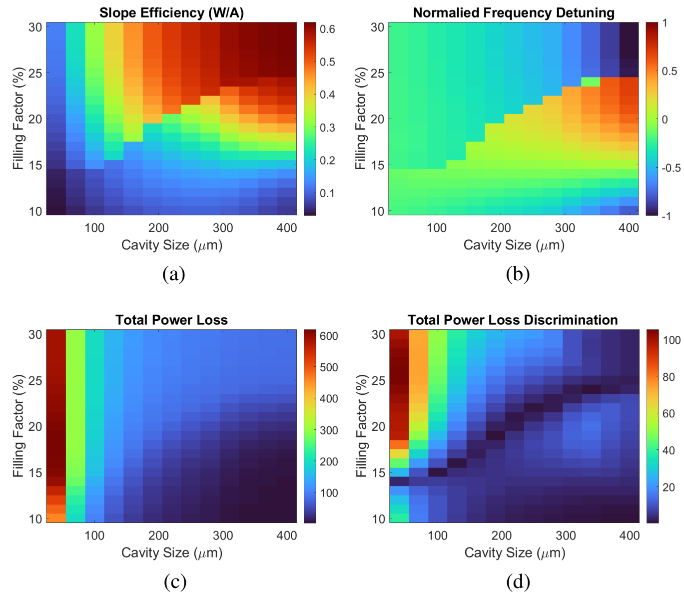

Fig. 3: The (a) slope efficiency, (b) normalized frequency detuning, (c) modal power loss, and (d) loss discrimination of the threshold mode in the RIT-PCSEL

IV. Conclusions

An efficient eigenmode solver for simulating finite-size PCSELs has been demonstrated. The dependence of the investigated parameters on the output characteristics can therefore be analyzed comprehensively. It is advantageous to speed up the optimum design for epitaxial structure, PC pattern and fill factor, or other fabrication conditions.

References

[1] R. Morita et al., “High-Speed High-Power Free-Space Optical Communication via Directly Modulated Watt-Class Photonic-Crystal Surface-Emitting Lasers.” Optica, vol. 11, pp. 971-979, 2024.

[2] Y. Liang, C. Peng, K. Sakai, S. Iwahashi, and S. Noda, “Three-Dimensional Coupled-Wave Analysis for Square-Lattice Photonic Crystal Surface Emitting Lasers with Transverse-Electric Polarization: Finite-Size Effects,” Opt. Express, vol. 20, pp. 15945-15961, 2012.

[3] T. M. Huang, W. J. Chang, Y. L. Huang, W. W. Lin, W. C. Wang, and W. C. Wang, ”Preconditioning bandgap eigenvalue problems in three-dimensional photonic crystals simulations,” J. Comput. Phys., vol. 229, pp. 8684-8703, 2010.

[4] Z.-X. Yang, C.-Y. Kuo, and G. Lin, “Simulation of photonic-crystal surface-emitting lasers with air-hole and air-pillar structures,” Photonics, vol. 8, p. 189, 2021.